Chapter 6

Numerical Scheme with Convergence for a Generalized Time-Fractional Telegraph-Type Equation

6.1 Introduction

In last three decades, the subject of fractional calculus has a lengthy antiquity and has been found many applications in areas of engineering and science. In recent studies, it is observed that the interest of researchers in fractional calculus has been increasing continuously due to its wide applications in various fields. Development summaries of fractional calculus can be found in Podlubny [2], Kilbas et al. [5], and Sabatier et al. [6]. Fractional differential equations have attracted many researchers to model systems in various domains more accurately. Fractional Telegraph equations have been one among these fractional models. Telegraph equation is a partial differential equation applicable in several fields such as signal analysis [211], wave propagation [212] and anomalous diffusion [213] and many others could be found in the literature. Fractional telegraph equation is the telegraph equation where the integer order partial space and/or time derivative terms are replaced with certain fractional derivative. Fractional telegraph equations are chosen by many researchers in recent years due to its physical relevance [213, 214, 215, 216, 217, 218]. The different aspects of fractional telegraph equations to better understand the anomalous diffusion process in a blood flow experiment are studied by the authors in [213]. In [214], Dehghan and Lakestani solved the telegraph equation using the Chebyshev cardinal function. Chen et al. [215] derived the analytical solution of time-fractional telegraph equation by the method of separation of variables. Orsingher and Beghin studied the fundamental solutions of time fractional telegraph equations of order 2α [216]. In [217], Beghin and Orsingher considered fractional telegraph equation with partial fractional derivatives of rational order $\alpha = m/n$ with $m < n$. Momani [218] discussed the analytic and approximate solutions of space and time fractional telegraph equation using Adomian decomposition. Yousefi [219] used the Legendre multiwavelet Galerkin method for solving the hyperbolic telegraph equation. Some more methods such as meshless methods [220, 221, 222, 223], variational iteration method [224] are also discussed for time fractional Telegraph equations with different boundary conditions. Fractional telegraph equations in higher dimensions are also studied by the researchers in recent years. These works include the spectral meshless radial point interpolation methods [225, 226], meshless RBF method [227], and least squares approximation [228]. Asgari et al. [229] applied the Bernstein polynomials operational matrices method to get the numerical solution of telegraph equation. Dehghan and Shokri [230] considered the thin plate splines radial basis functions for the numerical solution of the hyperbolic telegraph equation. Fractional Telegraph equations can be considered as a fractional partial differential equations thus operational matrix approach [195], homotopy analysis method for fractional partial differential equations [231] and discretization schemes [153] can also be investigated for such equations. Due to the multiple terms of partial derivatives in equation, it is not easy, even not possible, to deduce the analytical solution. Therefore, numerical methods including finite difference, finite element and spectral methods are discussed in numerical fractional PDEs [156].

In this chapter, we consider the time fractional telegraph equation in term of generalized fractional derivative defined in Caputo sense and present a numerical scheme for solving it. The generalized fractional derivative was proposed in [83], and it contains a scale function and a general weight in formulation. Later, it is applied to fractional Burgers equation, advection-diffusion equations then more interesting dynamics and properties depending on the related scale and weight functions are analysed [102, 232, 233]. This motivates us to further study telegraph equation with the same generalized fractional derivative. We shall discuss the dependence of numerical solutions of generalized telegraph-type equation on scale function, weight function, as well as order of fractional derivative. When certain parameters and settings are chosen, the abovementioned generalized telegraph equation reduces to conventional fractional counterpart, or classic telegraph equations. The structure of this chapter is as follows. We begin by introducing some basic definitions and mathematical background of the fractional calculus theory which are required for establishing our results. In Section 6.2, we discuss the problem formulation and its computational algorithm. In Section 6.3, we present the stability and convergence of numerical scheme. Section 6.4 includes three examples to show the efficiency and simplicity of the method. In Sections 6.5 and 6.6, we discuss the effect of scale and weight functions to the numerical solution of the problem.

6.2 Problem Formulation and Computational Algorithm

A Telegraph equation (TE) is a partial differential equation defined in term of space and time variables. A fractional Telegraph equation (FTE) is obtained by replacing integer order partial space and /or time derivative terms with fractional counter parts derivative. In a recent work [216], Orsingher and Beghin presented a study of the fractional telegraph equation given by,

$$\frac{\partial u(x,t)}{\partial t} + 2\lambda \frac{\partial^{1/2} u(x,t)}{\partial t^{1/2}} = c^2 \frac{\partial^2 u(x,t)}{\partial x^2} \tag{6.1}$$

$$u(x,t) = \varphi(x), \quad x \in \mathbb{R}, \; t > 0.$$

Orsingher and Beghin discussed that the general solution of Eq.(6.1) coincides with the distribution of the telegraph process whose time is an independent reflecting Brownian motion. Here, we discuss a formulation for the GTFTTE, and develop a numerical scheme for solving it. Further, we investigate the stability and convergence of the numerical scheme.

The Generalized Time Fractional Partial Derivative (GTFPD) which reduces in Caputo derivative in special choice of scale and weight functions. In order to define GTFTTE, we define GTFPD of type 2 with order $\alpha (0 < \alpha < 1)$, in the Caputo sense as,

$$\frac{{}^{*}\partial^{\alpha} u(x,t)}{{}^{*}\partial t^{\alpha}} = \frac{[w(t)]^{-1}}{\Gamma(1-\alpha)} \int_0^t \frac{1}{[z(t) - z(\tau)]^{\alpha}} \frac{\partial}{\partial \tau} [w(\tau) u(x,\tau)] d\tau. \tag{6.2}$$

Now replacing the fractional derivative term in Eq.(6.1) by the GTFFD as presented above in Eq.(6.2), we get a new form of Eq.(6.1) as with force term $f(x,t)$ as,

$$\frac{{}^*\partial^\alpha u(x,t)}{{}^*\partial t^\alpha} + \frac{\partial u(x,t)}{\partial t} = \frac{\partial^2 u(x,t)}{\partial x^2} + f(x,t) \tag{6.3}$$

with the following initial and boundary conditions,

$$u(x,0) = \varphi(x), \quad x \in [a,b], \tag{6.4}$$

$$u(a,t) = u(b,t) = 0, \quad t > 0, \quad 0 < \alpha < 1. \tag{6.5}$$

Note that Eq.(6.3) could be considered as the generalized form of Eq.(6.1) and it reduces to Eq.(6.1) for weight function $w(t) = 1$ and $z(t) = t, f(x,t) = 0$. We name this type of fractional Telegraph type equation defined by Eq. (6.3) as Generalized Time Fractional Telegraph Type Equation (in short GTFTTE).

In order to describe a numerical scheme, we divide time and space domain into M and N equal parts respectively, such that $\Delta t = T/M$ and $\Delta x = (b-a)/N$, where Δt and Δx are the time and space grid spacing, respectively. We label the space nodes as $x_i = a + i(\Delta x), i = 0, 1, \ldots, N$ such that $x_0 = a$ and $x_N = b$ are the boundary nodes, and the time nodes as $t_j = j(\Delta t), j = 0, 1, \ldots, M$, where $t_0 = 0$ is the initial time. For convenience, we denote $u(x_i, t_j) = u_j^i, w(t_j) = w_j$ and $z(t_j) = z_j$. For numerical solution, we approximate each term of GTFTTE by Eq.(6.3). Firstly, we approximate the first term of Eq.(6.3) as follows

$$\left[\frac{{}^*\partial^\alpha u(x,t)}{{}^*\partial t^\alpha}\right]_{(x_i,t_{j+1})} = \frac{[w(t)]^{-1}}{\Gamma(1-\alpha)} \int_0^{t_{j+1}} \frac{\frac{\partial}{\partial \tau}[w(\tau)u(x_i,\tau)]}{[z(t_{j+1}) - z(\tau)]^\alpha} d\tau.$$

$$\approx \frac{[w(t_{j+1})]^{-1}}{\Gamma(1-\alpha)} \sum_{k=0}^{j} \int_{t_k}^{t_{k+1}} \frac{w(t_{k+1})u(x_i,t_{k+1}) - w(t_k)u(x_i,t_k)}{(t_{k+1}-t_k)[z(t_{j+1}) - z(\tau)]^\alpha} d\tau,$$

$$\approx \frac{[w_{j+1}]^{-1}}{\Gamma(2-\alpha)} \sum_{k=0}^{j} \frac{w_{k+1}u^i_{k+1} - w_k u^i_k}{(t_{k+1}-t_k)} \left[(z_{j+1}-z_k)^{1-\alpha} - (z_{j+1}-z_{k+1})^{1-\alpha}\right]. \tag{6.6}$$

We use finite difference scheme to classical first order and second order derivative of$u(x,t)$ with respect to t and x in Eq.(6.3) respectively as,

$$\left[\frac{\partial u(x,t)}{\partial t}\right]_{(x_i,t_{j+1})} \approx \frac{u(x_i,t_{j+1}) - u(x_i,t_j)}{\Delta t} = \frac{u^i_{j+1} - u^i_j}{\Delta t} \tag{6.7}$$

$$\left[\frac{\partial^2 u(x,t)}{\partial t^2}\right]_{(x_i,t_{j+1})} \approx \frac{u(x_{i+1},t_{j+1}) - 2u(x_i,t_{j+1}) - u(x_{i-1},t_{j+1})}{(\Delta x)^2} = \frac{u^{i+1}_{j+1} - 2u^i_{j+1} + u^{i-1}_{j+1}}{(\Delta x)^2}. \tag{6.8}$$

Putting the approximations from Eqs.(6.6)-(6.8) into Eq.(6.3), we have

$$\begin{aligned}\frac{[w_{j+1}]^{-1}}{\Gamma(2-\alpha)} \sum_{k=0}^{j} \frac{w_{k+1}u^i_{k+1} - w_k u^i_k}{(z_{k+1}-z_k)} &[(z_{j+1}-z_k)^{1-\alpha} - (z_{j+1}-z_{k+1})^{1-\alpha}] \\ + \left[\frac{u^i_{j+1} - u^i_j}{\Delta t}\right] + \left[\frac{u^{i+1}_{j+1} - 2u^i_{j+1} - u^{i-1}_{j+1}}{(\Delta x)^2}\right] &+ f^i_{j+1}.\end{aligned} \tag{6.9}$$

For simplicity of calculation Eq.(6.9) can be written in the following form,

$$\mu(u^{i+1}_{j+1} - 2u^i_{j+1} - u^{i-1}_{j+1}) - \xi(u^i_{j+1} - u^i_j) = \sum_{k=0}^{j}(s^j_k u^i_{k+1} - v^j_k u^i_k) - f^i_{j+1}, \tag{6.10}$$

for $0 \le j \le M-1$ and $0 \le i \le N-1$,

where,

$$s^j_k = \frac{w^{-1}_{j+1} w_{k+1}}{\Gamma(2-\alpha)(z_{k+1}-z_k)}[(z_{j+1}-z_k)^{1-\alpha} - (z_{j+1}-z_{k+1})^{1-\alpha}] \tag{6.11}$$

$$v^j_k = \frac{w^{-1}_{j+1} w_k}{\Gamma(2-\alpha)(z_{k+1}-z_k)}[(z_{j+1}-z_k)^{1-\alpha} - (z_{j+1}-z_{k+1})^{1-\alpha}] \tag{6.12}$$

$$\xi = \frac{1}{\Delta t}. \tag{6.13}$$

$$\mu = \frac{1}{(\Delta x)^2}. \tag{6.14}$$

From initial conditions, we get $u_1^0 = u_1^N$, and Eq. (6.10) for $j = 0$ gives $u_1^i, 1 \leq i \leq N-1$. For $j \geq 1$, Eq.(6.10) can be written as,

$$\mu u_{j+1}^{i-1} + (-2\mu - s_j^j - \xi) u_{j+1}^i + \mu u_{j+1}^{i+1} = -v_j^j u_j^i - \xi u_j^i + \sum_{k=0}^{j-1} (s_k^j u_{k+1}^i - v_k^j u_k^i) - f_{j+1}^i. \quad (6.15)$$

Using $k_j^i = -2\mu - s_j^j - \xi$, we can write Eq.(6.10) in the following form as ,

$$K_{j+1} U_{j+1} = F_{j+1}, \quad 0 \leq j \leq M-1, \quad (6.16)$$

where

$$K_{j+1} = \begin{pmatrix} k_j^1 & \mu & & & & \\ \mu & k_j^2 & \mu & & & \\ & & \ddots & \ddots & \ddots & \\ & & & \mu & k_j^{N-2} & \mu \\ & & & & \mu & k_j^{N-1} \end{pmatrix}, \quad (6.17)$$

$$U_{j+1} = [u_{j+1}^1, u_{j+1}^2, ..., u_{j+1}^i, ..., u_{j+1}^{N-1}]^T, \ u_j^0 = u_j^N = 0, \quad (6.18)$$

$$F_{j+1} = [F_{j+1}^1, F_{j+1}^2, ..., F_{j+1}^i, ..., F_{j+1}^{N-1}]^T, \quad (6.19)$$

and

$$F_{j+1}^i = \begin{cases} -v_0^0 u_0^i - \xi u_0^i - f_1^i, & \text{for} \quad j = 0 \\ -v_j^j u_j^i - \xi u_j^i + \sum_{k=0}^{j-1} (s_k^j u_{k+1}^i - v_k^j u_k^i) - f_{j+1}^i, & \text{for} \quad 1 \leq j \leq M-1. \end{cases} \quad (6.20)$$

Again in order to proof the stability of numerical scheme, we can easily check that the coefficients s_k^j and v_k^j have the following properties:

Lemma 6.2.1. *Suppose that $0 < \alpha < 1$, and the scale function $z(t)$ is non-negative and strictly monotone increasing, and the weight function $w(t)$ is positive and monotone increasing. Under these conditions, the following conclusions hold:*

(i) $s_k^j > v_k^j > 0$ and $w_k s_k^j = w_{k+1} v_k^j$, and

(ii) if w(t) is a nonzero constant,then $s_k^j = v_k^j$ for all k=0,1,2,...,j.

6.3 Stability and Convergence Analysis

To describe the stability and convergence analysis of the presented scheme for Eq.(6.3), the following theorem is required.

Theorem 6.3.1. *(Lax-Richertmyer theorem, ([122]) if the differential Eq.(6.3) is well-posed and the finite difference method is consistent, then the finite difference method is convergent if and only if, it is stable.*

Theorem 6.3.2. *Suppose that the scale function $z(t)$ is monotone increasing and positive, weight $w(t)$ is nondecreasing and positive, then the full discretization scheme as given in Eq. (6.10) is sable, and hence is convergent.*

Proof: To study the stability of the numerical scheme (6.10), it is sufficient to prove the stability of its homogeneous iteration scheme, i.e. the stability is independent of right side function $f(x,t)$ in Eq.(6.3). Thus we take the solution of the form $u_{j+1}^m = \delta_{j+1} e^{i\theta m y}, i = \sqrt{-1}$ (we note that only in this proof, i means the unit of complex number.), θ is a real number, $1 \leq m \leq N-1$. Hence the homogeneous iteration scheme of Eq.(6.10) becomes

$$\begin{aligned}
&\mu\delta_{j+1}e^{i\theta(m-1)y} + (-2\mu - s_j^j - \xi)\delta_{j+1}e^{i\theta my} + \mu\delta_{j+1}e^{i\theta(m+1)y} \\
&= -v_j^j\delta_j e^{i\theta my} - \xi\delta_j e^{i\theta my} + \sum_{k=0}^{j-1}(s_k^j\delta_{j+1}e^{i\theta my} - v_k^j\delta_j e^{i\theta my}).
\end{aligned} \tag{6.21}$$

This implies,

$$\begin{aligned}
&-\mu\delta_{j+1}e^{-i\theta y} - (2\mu + s_j^j + \xi)\delta_{j+1} - \mu\delta_{j+1}e^{i\theta y} \\
&= v_j^j\delta_j + \xi\delta_j - \sum_{k=0}^{j-1}(s_k^j\delta_{j+1} - v_k^j\delta_j).
\end{aligned}$$

$$\begin{aligned}
&\mu\delta_{j+1}(-e^{-i\theta y} + 2 - e^{i\theta y}) + s_j^j\delta_{j+1} + \xi\delta_{j+1} \\
&= v_j^j\delta_j + \xi\delta_j - \sum_{k=0}^{j-1}(s_k^j\delta_{j+1} - v_k^j\delta_j).
\end{aligned}$$

$$\begin{aligned}
&(2\mu - 2\mu\cos\theta y)\delta_{j+1} + s_j^j\delta_{j+1} + \xi\delta_{j+1} \\
&= v_j^j\delta_j + \xi\delta_j - \sum_{k=0}^{j-1}(s_k^j\delta_{j+1} - v_k^j\delta_j).
\end{aligned} \tag{6.22}$$

From Lemma 6.2.1, we have $s_k^j \geq v_k^j$ for all $k = 0, 1, 2, \ldots, j$ and $j = 0, 1, 2, \ldots, M-1$. Hence, from Eq.(6.22), we get

$$\begin{aligned}
\delta_{j+1} &= \frac{v_j^j\delta_j + \xi\delta_j - \sum_{k=0}^{j-1}(s_k^j\delta_{j+1} - v_k^j\delta_j)}{(2\mu - 2\mu\cos\theta y) + s_j^j + \xi} \\
&= \frac{(v_j^j + \xi)\delta_j}{[2\mu - 2\mu\cos\theta y] + s_j^j + \xi} - \frac{\sum_{k=0}^{j-1}(s_k^j\delta_{j+1} - v_k^j\delta_j)}{[2\mu - 2\mu\cos\theta y] + s_j^j + \xi} \\
&\leq \frac{(v_j^j + \xi)\delta_j}{(s_j^j + \xi)} - \frac{\sum_{k=0}^{j-1}(s_k^j\delta_{j+1} - v_k^j\delta_j)}{[2\mu - 2\mu\cos\theta y] + s_j^j + \xi} \leq \delta_j.
\end{aligned} \tag{6.23}$$

6.4 Numerical Results and their Analysis

Here, we discuss three examples to investigate the validity of proposed numerical scheme. We also conduct the numerical experiments by varying the scale function and weight functions. We also present the numerical results to verify the stability of the numerical method.

Example 6.4.1. *Consider Eq.(6.3) with the following initial and boundary conditions,*

$$u(x,0) = 0, x \in [0,1], u(0,t) = u(1,t) = 0, t > 0.$$

The force term is $f(x,t) = 2x(x-1)[\frac{t^{2-\alpha}}{\Gamma(3-\alpha)} + t] - 2t^2$. In this case, the exact solution of Eq.(6.3) is given by $u(x,t) = x(x-1)t^2$.

We solve Eq.(6.3) by the presented numerical scheme with different step sizes.The exact and numerical solutions are presented for $\alpha = 0.8, 0.5$ in Figures 6.1-6.2 with $z(t) = t, w(t) = 1$.

For study the numerical convergence order of the numerical scheme, we solve Example 6.4.1 with different step sizes. The convergence order (CO) is calculated numerically. The maximum absolute errors (MAE) and convergence order are shown in Table 6.1 and Table 6.2 for $\alpha = 0.8$ and $\alpha = 0.5$ respectively. Numerical outcomes of this example show that the numerical scheme is stable and we conclude that the convergence order of numerical scheme goes to one as the step size reduces, which suggests that numerical scheme is a first-order scheme. It is also clear from table the CO order is not dependent on α.

TABLE 6.1: MAE and CO of Example 6.4.1 with $\alpha = 0.8$.

Δt	Δx	MAE	CO
1/8	1/8	0.0539	
1/16	1/16	0.0280	0.944858
1/32	1/32	0.0143	0.969412
1/64	1/64	0.0072	0.989946
1/128	1/128	0.0036	1.00000
1/256	1/256	0.0018	1.00000
1/512	1/512	0.000916	0.974577
1/1024	1/1024	0.00046	0.993714

TABLE 6.2: MAE and CO of Example 6.4.1 with $\alpha = 0.5$.

Δt	Δx	MAE	CO
1/8	1/8	0.0551	
1/16	1/16	0.0286	0.946037
1/32	1/32	0.0146	0.970047
1/64	1/64	0.0073	1.00000
1/128	1/128	0.0037	0.980371
1/256	1/256	0.0019	0.961526
1/512	1/512	0.000927	1.0307
1/1024	1/1024	0.00046	1.0156

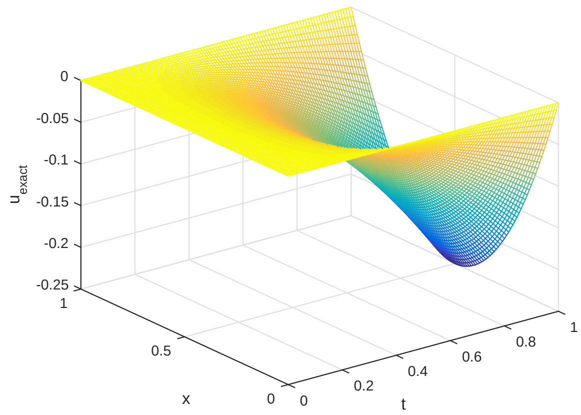

FIGURE 6.1: Exact solution for Example 6.4.1.

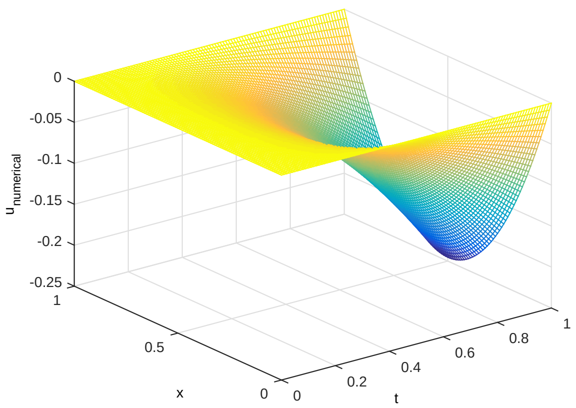

$\alpha = 0.8, \Delta x = 0.01, \Delta t = 0.01.$

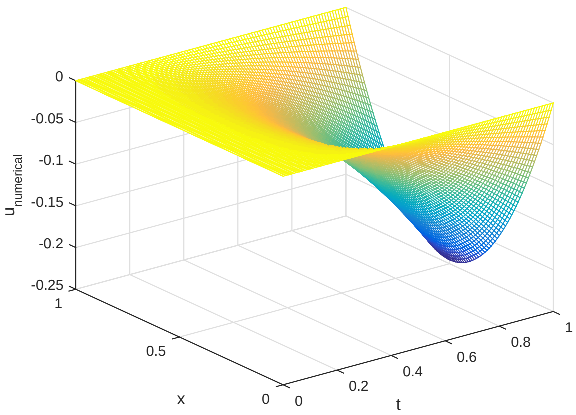

$\alpha = 0.5, \Delta x = 0.01, \Delta t = 0.01.$

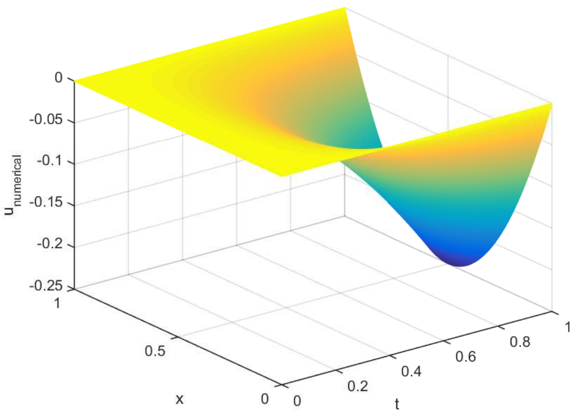

$\alpha = 0.5, \Delta x = 0.001, \Delta t = 0.001.$

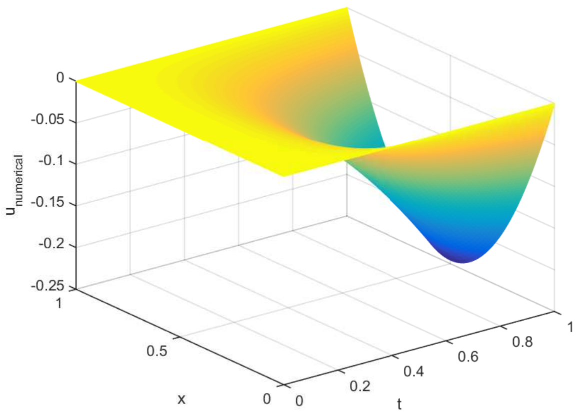

$\alpha = 0.5, \Delta x = 0.001, \Delta t = 0.01.$

FIGURE 6.2: Numerical solutions of Example 6.4.1 with different step size and fractional orders.

Example 6.4.2. *Consider Eq.(6.3) with the following initial and boundary conditions,*

$$u(x,0) = \sin(2\pi x), x \in [0,1], u(0,t) = u(1,t) = 0, t > 0.$$

The force term is $f(x,t) = \frac{2x(x-1)t^{2-\alpha}}{\Gamma(3-\alpha)} + 2x(x-1)t + 4\pi^2 \sin(2\pi x) - 2t^2$. In this case, the exact solution of Eq.(6.3) is given by $u(x,t) = \sin(2\pi x) + x(x-1)t^2$.

Figures 6.3-6.4 show the exact solution and numerical solutions of the Example 6.4.2 when $\Delta x = 0.001, \Delta t = 0.01$ and $\Delta x = \Delta t = 0.001$ with $\alpha = 0.8, 0.5, z(t) = t$, $w(t) = 1$. In similar manner for study of the convergence order of Example 6.4.2 ,we solve the Example 6.4.2 with different step sizes. The maximum absolute errors and convergence order of this Example show that our numerical scheme is stable and of first-order. The maximum absolute errors and convergence order are shown in Table 6.3 and Table 6.4 for $\alpha = 0.8$ and $\alpha = 0.5$ respectively. Tables 6.5, 6.6, 6.7 and 6.8 present MAE and CO for $\alpha = 0.5$, and 0.8 with 1) varying Δt and fixing Δx, and 2) varying Δx with fixing Δt. Tables 6.5-6.8 show that convergence order in temporal direction is one while convergence order in spatial direction is two and validates the theoretical results of finite difference scheme.

TABLE 6.3: MAE and CO of Example 6.4.2 with $\alpha = 0.8$.

Δt	Δx	MAE	CO
1/8	1/8	0.0932	
1/16	1/16	0.0360	1.37233
1/32	1/32	0.0157	1.19723
1/64	1/64	0.0074	1.08517
1/128	1/128	0.0037	1.00000
1/256	1/256	0.0018	1.03953
1/512	1/512	0.00092	0.96829
1/1024	1/1024	0.00045	1.03171

TABLE 6.4: MAE and CO of Example 6.4.2 with $\alpha = 0.5$.

Δt	Δx	MAE	CO
1/8	1/8	0.0936	
1/16	1/16	0.0364	1.36257
1/32	1/32	0.0159	1.19491
1/64	1/64	0.0075	1.08406
1/128	1/128	0.0037	1.01937
1/256	1/256	0.0019	0.961526
1/512	1/512	0.00093	1.0307
1/1024	1/1024	0.000464	1.0031

Table 6.5: MAE and CO for Example 6.4.2 with different Δt and fixing $\alpha = 0.5, \Delta x = 1/512$.

Δt	MAE	CO
$1/8$	0.0035	
$1/16$	0.0017	1.0418
$1/32$	0.00082	1.0518
$1/64$	0.0004	1.0356

Table 6.6: MAE and CO for Example 6.4.2 with different Δt and fixing $\alpha = 0.8, \Delta x = 1/512$.

Δt	MAE	CO
$1/8$	0.0047	
$1/16$	0.0022	1.0952
$1/32$	0.0011	1.000
$1/64$	0.00052	1.0809

Table 6.7: MAE and CO for Example 6.4.2 with different Δx and fixing $\alpha = 0.5, \Delta t = 1/512$.

Δt	MAE	CO
$1/8$	0.0522	
$1/16$	0.0128	2.0279
$1/32$	0.0032	2.000
$1/64$	0.00083	1.9469

TABLE 6.8: MAE and CO for Example 6.4.2 with different Δx and fixing $\alpha = 0.8, \Delta t = 1/512$.

Δt	MAE	CO
1/8	0.0527	
1/16	0.0129	2.0304
1/32	0.0032	2.0112
1/64	0.00084	1.9296

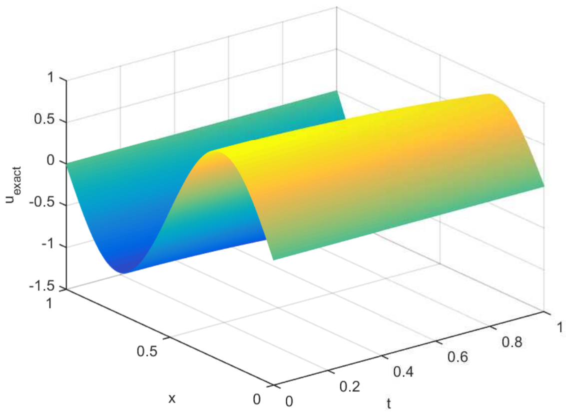

FIGURE 6.3: Exact solutions for Example 6.4.2

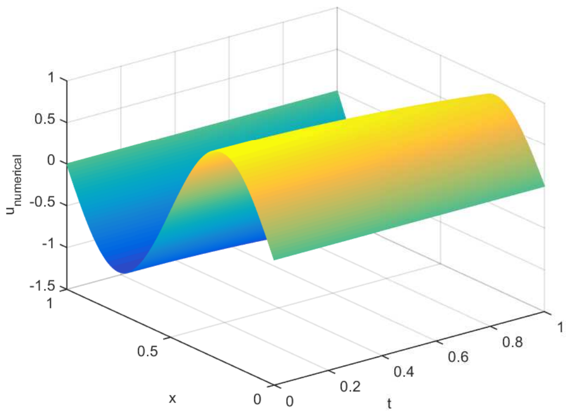

$\alpha = 0.8, \Delta x = 0.001, \Delta t = 0.01.$

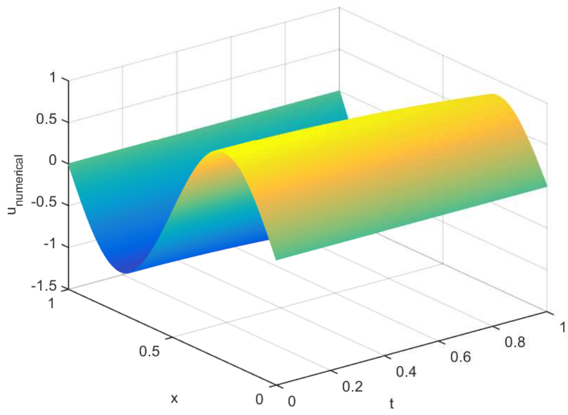

$\alpha = 0.8, \Delta x = 0.001, \Delta t = 0.001.$

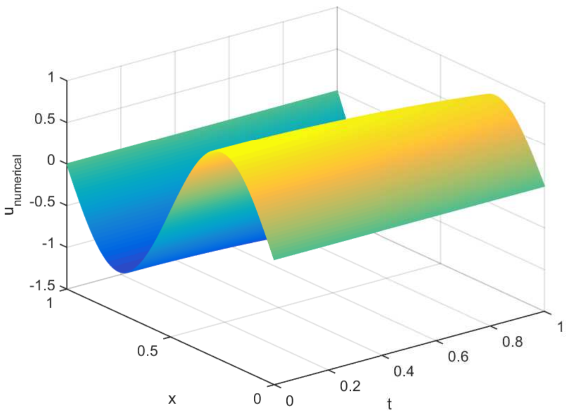

$\alpha = 0.5, \Delta x = 0.001, \Delta t = 0.001.$

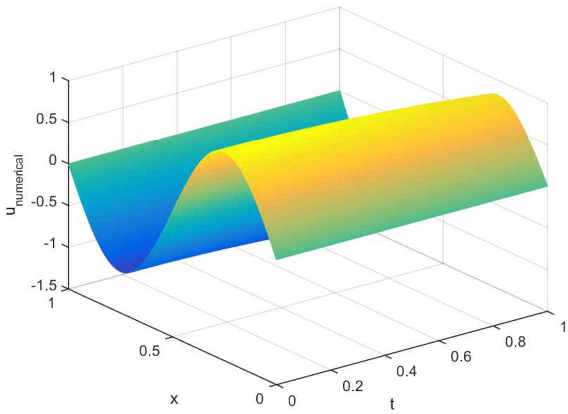

$\alpha = 0.5, \Delta x = 0.001, \Delta t = 0.01.$

FIGURE 6.4: Numerical solutions of Example 6.4.2 with different step size and fractional orders.

Example 6.4.3. *Consider Eq.(6.3) with the following initial and boundary conditions,*

$$u(x,0) = \sin(\pi x), x \in [0,1], u(0,t) = u(1,t) = 0, t > 0.$$

The force term is $f(x,t) = \frac{1}{\Gamma(1-\alpha)} \sin(\pi x) exp(-t) \{\Gamma(1-\alpha) - \gamma(1-\alpha,t)\} + (\pi^2 - 1)\sin(\pi x) exp(-t)$, where $\gamma(s,z)$ denotes the incomplete Gamma function. In this case, the exact solution of Eq.(6.3) is given by $u(x,t) = \sin(\pi x) exp(-t)$.

Figures 6.5-6.6 show the exact and numerical solutions of the Example 6.4.3 when $\Delta x = \Delta t = 0.01; \Delta x = \Delta t = 0.001; \Delta x = 0.001, \Delta t = 0.02$ and $\Delta x = 0.01, \Delta t = 0.02$ with $\alpha = 0.5, 0.8, z(t) = t, w(t) = exp(2t)$. For study of the convergence order of Example 6.4.3, we solve the Example 6.4.3 with different step sizes. The MAE and CO are shown in Table 6.9 and Table 6.10 for $\alpha = 0.5, \alpha = 0.8$ respectively. Tables 6.11, 6.12, 6.13, and 6.14 represent the MAE and CO for $\alpha = 0.5$ and $\alpha = 0.8$ with varying Δt and Δx.

TABLE 6.9: MAE and CO of Example 6.4.3 with $\alpha = 0.5$.

Δt	Δx	MAE	CO
1/8	1/8	0.0117	
1/16	1/16	0.0041	1.5128
1/32	1/32	0.0016	1.3576
1/64	1/64	0.0007	1.1926
1/128	1/128	0.0003	1.2224
1/256	1/256	0.00014	1.0995
1/512	1/512	0.00007	1.0000
1/1024	1/1024	0.000033	1.0849

TABLE 6.10: MAE and CO of Example 6.4.3 with $\alpha = 0.8$.

Δt	Δx	MAE	CO
1/8	1/8	0.0123	
1/16	1/16	0.0045	1.4507
1/32	1/32	0.0018	1.3219
1/64	1/64	0.0007	1.3626
1/128	1/128	0.0003	1.2224
1/256	1/256	0.00015	1.0000
1/512	1/512	0.00007	1.0995
1/1024	1/1024	0.000036	0.9594

TABLE 6.11: MAE and CO for Example 6.4.3 with different Δt and fixing $\alpha = 0.5, \Delta x = 1/512$.

Δt	MAE	CO
1/8	0.0043	
1/16	0.0022	0.9668
1/32	0.0011	1.0000
1/64	0.00054	1.0265

Table 6.12: MAE and CO for Example 6.4.3 with different Δt and fixing $\alpha = 0.8, \Delta x = 1/512$.

Δt	MAE	CO
1/8	0.0052	
1/16	0.0026	1.0000
1/32	0.0013	1.0000
1/64	0.00063	1.0451

Table 6.13: MAE and CO for Example 6.4.3 with different Δx and fixing $\alpha = 0.5, \Delta t = 1/512$.

Δt	MAE	CO
1/8	0.0084	
1/16	0.0021	2.0000
1/32	0.00058	1.8563
1/64	0.00019	1.6101

Table 6.14: MAE and CO for Example 6.4.3 with different Δx and fixing $\alpha = 0.8, \Delta t = 1/512$.

Δt	MAE	CO
1/8	0.0079	
1/16	0.0020	1.9819
1/32	0.00056	1.8365
1/64	0.00019	1.5594

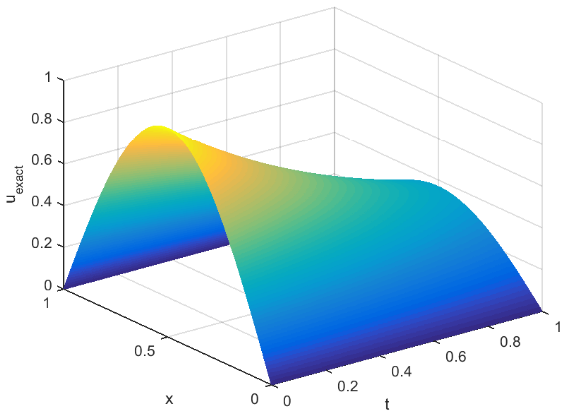

FIGURE 6.5: Exact solution for Example 6.4.3

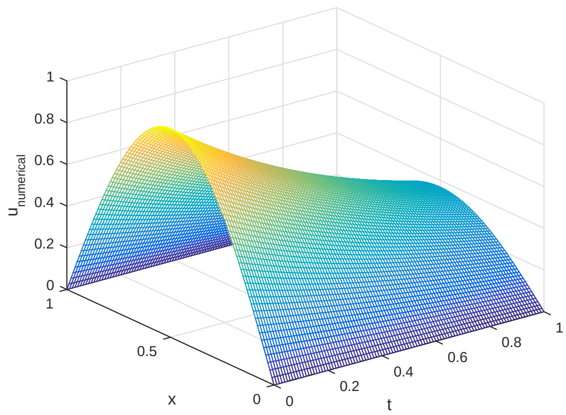

$\alpha = 0.5, \Delta x = 0.01, \Delta t = 0.01.$

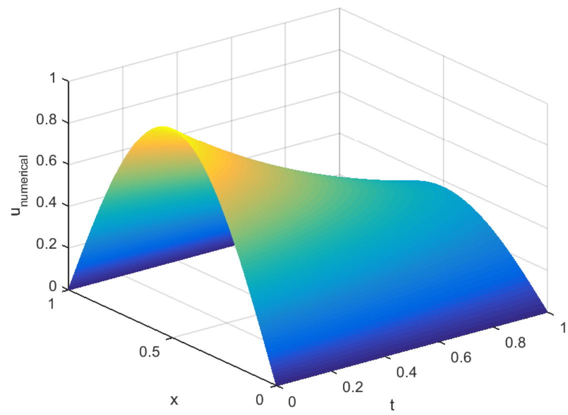

$\alpha = 0.5, \Delta x = 0.001, \Delta t = 0.001.$

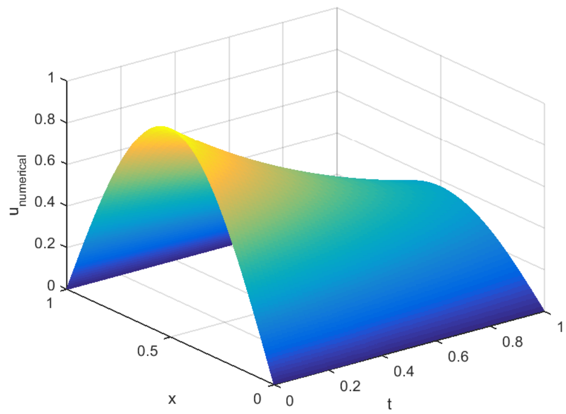

$\alpha = 0.8, \Delta x = 0.001, \Delta t = 0.02.$

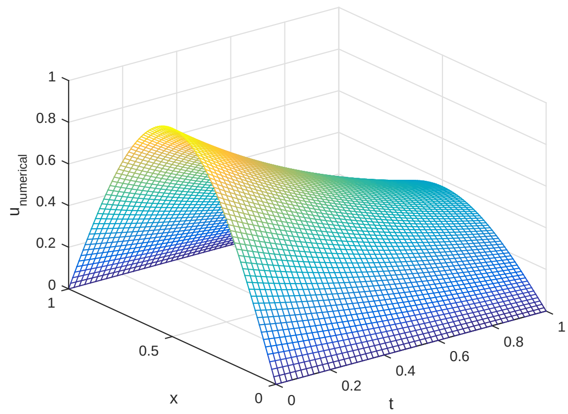

$\alpha = 0.8, \Delta x = 0.01, \Delta t = 0.02.$

FIGURE 6.6: Numerical solutions of Example 6.4.3 with different step size and fractional orders.

6.5 Effect of Scale Function *z(t)*

To analyse the behaviour of the numerical solution with scale function $z(t)$, we consider $z(t)$ to be monotonic function. For the monotonic increasing scale function, the time domain $(0, T)$ shifted to $(z(0), z(T))$ by scale function and for decreasing scale function, it shifted to interval $(z(T), z(0))$. Due to this, we consider two types of scale functions namely, monotonic contraction and stretching. For the effect of scale function, we take weight function $w(t) = 1$. For numerical descriptions, we take $\Delta x = \Delta t = 0.01, \alpha = 0.8, z(t) = t^2, t^3, t^5, t^{0.5}, t^{0.9}$ and $20t$ in Example 6.4.1. The first five and last one functions represent the nonlinear and the linear scale functions, respectively. The numerical simulation depicts the behaviour of solution is either stretching or contracting according to scale function. The results for these conditions, parameters and functions are presented in Figures 6.7, 6.8, 6.9, 6.10, 6.11 and 6.12.

Case 1: In this case, scale function shows a "contracting function" with a uniform contract time domain $[0, 1]$. It is clear from Figures 6.7, 6.8 and 6.9, which is numerical simulation of Example 6.4.1 the behaviour of solution is stretching whenever the scale function are taken contracting.

Case 2: In this case, scale function depicts a "stretching function" with variable stretch over the domain $[0, 1]$. It is clear from Figures 6.10 and 6.11, the behaviour of solution is contracting whenever the scale function are taken stretching.

Hence, solution of GTFTTE is inversely affected to the behaviour of scale function both in the sense of stretching and contracting. Figure 6.12 also shows that when, scale function $z(t) = 20t$ has linear "stretching function" then solution of TE is stretching. Figures 6.10 and 6.11. also presented the merit of scale function when scale function $z(t) = t^{\beta}, 0 < \beta \leq 1$ approaches to $z(t) = t$ that is $\beta \to 1$ then it approach the solution of TE in Example 6.4.1.

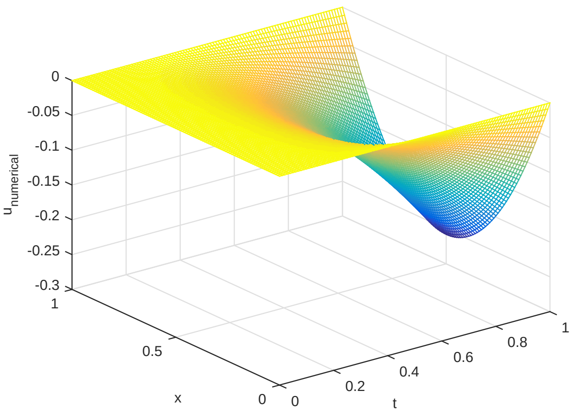

FIGURE 6.7: $z(t) = t^2$

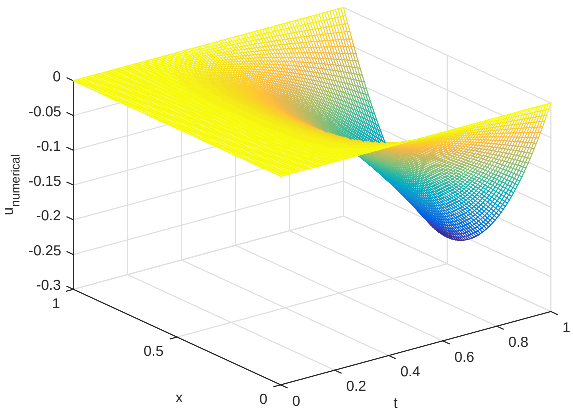

FIGURE 6.8: $z(t) = t^3$

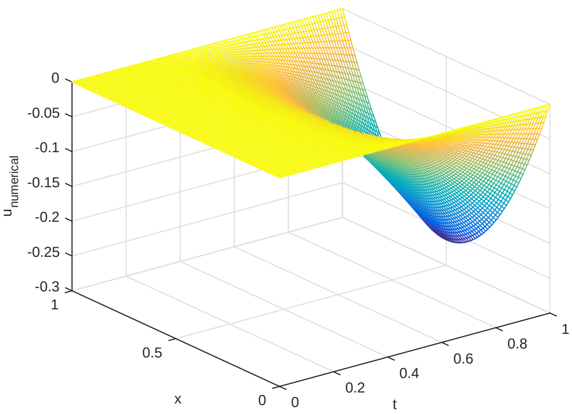

FIGURE 6.9: $z(t) = t^5$

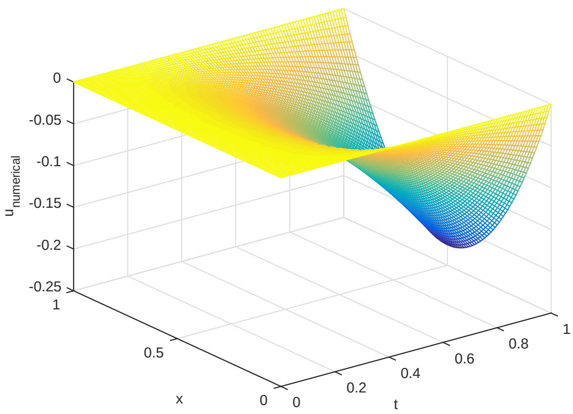

FIGURE 6.10: $z(t) = t^{0.5}$

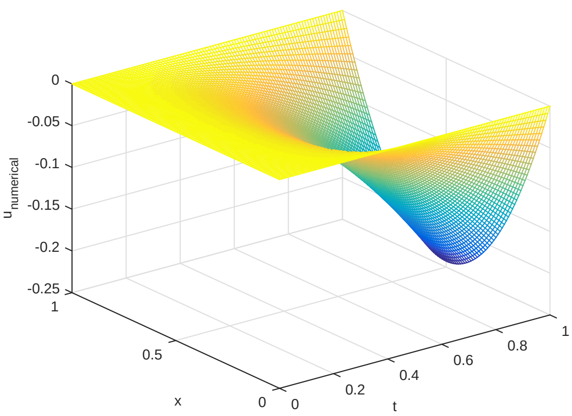

FIGURE 6.11: $z(t) = t^{0.9}$

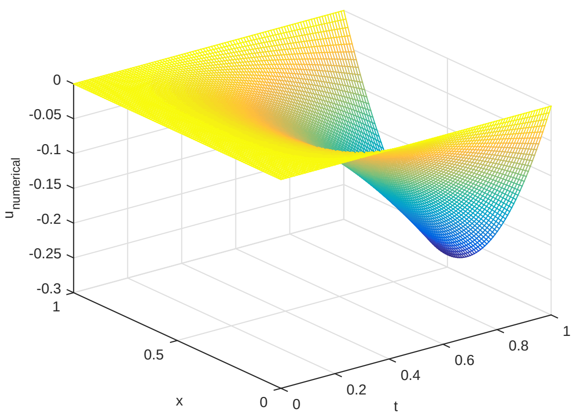

FIGURE 6.12: $z(t) = 20t$

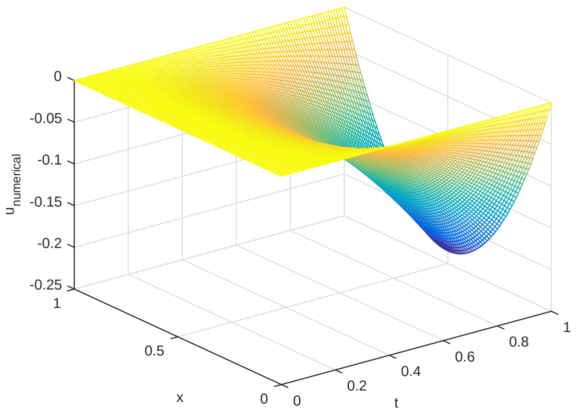

FIGURE 6.13: $w(t) = exp(t)$

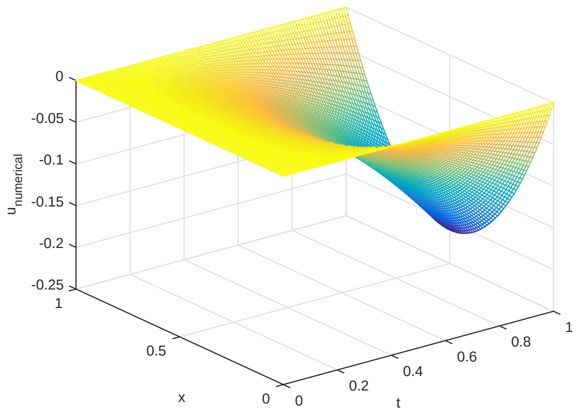

FIGURE 6.14: $w(t) = exp(4t)$

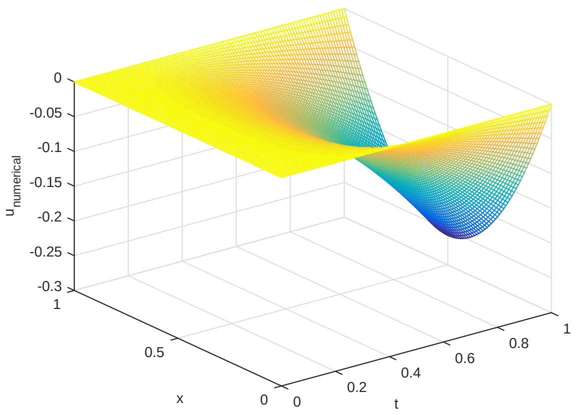

FIGURE 6.15: $w(t) = exp(-t)$

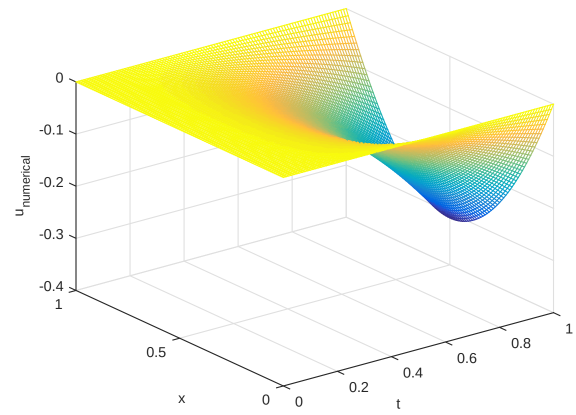

FIGURE 6.16: $w(t) = exp(-4t)$

6.6 Effect of Weight Function *w(t)*

To study the effect of weight function $w(t)$ on the GTFTTE, we take scale function $z(t) = t$. For numerical simulation, we take $\Delta x = \Delta t = 0.01, \alpha = 0.8, w(t) = exp(t), exp(4t)$, $exp(-t)$ and $exp(-4t)$ for Example 6.4.1. According to numerical results, we observe the phenomena of weight functions. The solution of GTFTTE is directly affected to the behaviour of weight function in the sense of increasing and decreasing behaviour of weight functions. If we increase the weight function then solution is shifted upward direction that is the value of solution increase and for decreasing weight function, solution is shifted downward direction that is the value of solution decreases . The results for above conditions, parameters and functions are presented in Figures 6.13, 6.14, 6.15 and 6.16.

6.7 Conclusions

We studied a new generalized time-fractional telegraph type equation and discussed a numerical scheme based on finite difference method for solving it. The generalized fractional derivative is considered in Caputo sense and it depends on a scale function $z(t)$ and a weight function $w(t)$. The stability and convergence of the numerical scheme are also proved. To check the validity of numerical scheme, we take three examples and perform numerical simulations. Simulation results show that numerical scheme is of first order and stable. However, in specific direction such as special direction the scheme delivers second order convergence and in temporal direction it produces first order convergence. However, in specific direction such as temporal direction it produces first order convergence. We investigated the effect of the scale and weight functions on the telegraph type equation. The effects of weight functions are directly however, scale function is inversely to the solution of telegraph type equation. The numerical convergence orders and absolute errors are also presented through various tables.

****